

**Table VI.** Reaction Products from the Halogen Competition Reactions

Solvent	Styrene adducts, <sup>a</sup> %	Phenylacetylene adducts, <sup>b</sup> %	$k_o/k_a$
H <sub>2</sub> O	40	60	0.7
70% H <sub>2</sub> O–MeOH	62.5	37.5	1.7
50% H <sub>2</sub> O–MeOH	88.2	11.8	7.5
MeOH	>99	<1	>10 <sup>2</sup>
HAc	>99	<1	2590 <sup>c</sup>

<sup>a</sup> Dibromide and solvent incorporated products. <sup>b</sup> Mono- and dibromo ketones; it is assumed that enolic monobromides react much faster than either styrene or phenylacetylene and hence consumption of a second molecule of Br<sub>2</sub> by these species does not affect the competition. <sup>c</sup> Ratio calculated from actual rate constants.

**Competition Rate Ratios.** Into a 250–5000-ml one-necked flask was placed a predetermined volume of solvent saturated with oxy-

gen, styrene (2.60 mmol), and phenylacetylene (2.60 mmol). The solution was mixed and the flask covered to exclude light. A competitive amount (2.50 mmol) of a bromine solution was added dropwise and with stirring over a 15 min period. The solution was then extracted twice with pentane and the extract dried (MgSO<sub>4</sub>). The organic layer was condensed and product analysis was accomplished by glc and nmr. Products were determined by the  $\alpha$ - or  $\beta$ -proton resonances for the styrene adducts and by the ortho benzene ring protons of the ketones or the olefinic proton resonance of the acetylene adduct where appropriate. Table VI summarizes the products formed in each competitive reaction.

In order to establish the stability of the products in water and to discount any possible product equilibrium which could be present a control experiment was performed. Styrene and bromine were reacted in an aqueous medium. After the reaction was complete, phenylacetylene was added and stirred for 1 hr. The reaction mixture was worked-up and analyzed by nmr. The product distribution revealed that under the conditions of the competition reactions, the products formed were stable and no product equilibrium existed between olefin and acetylene.

**Acknowledgments.** The continued financial support of the National Research Council of Canada is gratefully acknowledged.

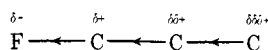
## The Conformational Dependence of the Inductive Effect in the $\sigma$ -Electron System as Studied by Carbon-13 Nuclear Magnetic Resonance

Isao Morishima,<sup>\*1a</sup> Kenichi Yoshikawa,<sup>1a</sup> Koji Okada,<sup>1a</sup> Teijiro Yonezawa,<sup>1a</sup> and Kojitsu Goto<sup>1b</sup>

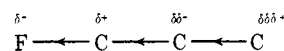
Contribution from the Department of Hydrocarbon Chemistry, Faculty of Engineering, Kyoto University, Kyoto, Japan, and JEOL Inc., Akishima, Tokyo, Japan. Received March 6, 1972

**Abstract:** The <sup>13</sup>C chemical shifts induced by the protonation in the trifluoroacetic acid solution have been measured for various aliphatic amines and N-heterocyclic six-membered ring compounds. The protonation-induced <sup>13</sup>C shifts are proved to exhibit marked structural and conformational dependences. These results are fairly well interpreted in terms of the charge densities on the carbon skeleton obtained by the semiempirical molecular orbital calculations and are discussed in relation to stereospecificity of the inductive effect in the  $\sigma$ -electron system.

Studies of the electronic inductive effect in the  $\pi$ -electron system have long been carried out experimentally and theoretically. However, the problem of the  $\sigma$ -inductive effect has been less studied. Elucidation of the structural and conformational dependences of the electronic structures of the  $\sigma$ -electron system is one of the essential problems in understanding various stereochemical problems in organic chemistry. The present study is concerned with delineating stereospecificity of the electronic inductive effect in the  $\sigma$ -electron system. A couple of decades ago, Ingold<sup>2</sup> suggested that an electron-withdrawing substituent, such as the fluorine atom, makes the atom of the  $\sigma$  skeleton positive, and that this effect is diminished gradually along the  $\sigma$  chain.



In contrast to this, Pople, *et al.*,<sup>3</sup> using the CNDO-SCF molecular orbital calculations, suggested that the inductive effect induced by such an electronegative substituent alternates and attenuates along the  $\sigma$  skeleton.



Although the concept of the  $\sigma$ -inductive effect has been well accepted in organic chemistry, the mode and mechanism of the transmission of the  $\sigma$ -inductive effect along the saturated molecules are still open to further experimental and theoretical investigations. In this sense, it seems worthwhile to examine experimentally these two aspects of the  $\sigma$  inductive effect and to investigate the consequences of conformational change in the  $\sigma$  skeleton.

It is well established that the <sup>13</sup>C chemical shift is quite a sensitive probe for detecting the structural and electronic perturbations around a carbon atom.

(3) J. A. Pople and M. S. Gordon, *J. Amer. Chem. Soc.*, **89**, 4253 (1967).

(1) (a) Kyoto University; (b) JEOL Inc.

(2) C. K. Ingold, "Structure and Mechanism in Organic Chemistry," G. Bell and Sons, London, 1953.

**Table I.**  $^{13}\text{C}$  Shifts of Free Amines ( $\delta^{13}\text{C}$ ) and N Protonation Shift ( $\Delta\delta^{13}\text{C}$ )

Molecules	Position	$\delta^{13}\text{C}^a$	$\Delta\delta^{13}\text{C},^b$ ppm	Molecules	Position	$\delta^{13}\text{C}^a$	$\Delta\delta^{13}\text{C},^b$ ppm
	2	143.5	+2.8		2	136.4	-0.2
	3	165.1	+4.8		3	157.8	+3.0
	4	166.9	+3.9		4	162.0	+2.2
	2	139.9	-2.6		7	146.1	+2.5
	3	157.4	+4.6		8	170.0	+1.9
	4	167.0	+3.5		2	129.6	-3.7
	5	165.9	+4.8		3	158.7	+2.7
	6	145.0	+1.2		4	167.4	+3.1
	7	169.4	+4.6		5	166.2	+2.6
	2	137.3	+3.1		2	144.6	+0.1
	3	160.2	+2.9		3	165.5	+4.4
	4	158.3	+3.7		4	171.5	+2.0
	5	165.5	+4.6		1	150.6	+2.8
	6	145.5	+1.0		2	156.1	+6.9
	7	172.9	+2.1		3	172.4	+0.8
	2	145.7	+0.9		4	178.8	+1.3
	3	156.6	+5.2		1	142.0	-2.7
	4	160.7	+2.8		2	155.3	+6.1
	7	169.9	+2.4		3	167.2	+1.2
	2	135.8	+0.1		4	166.4	+1.8
	3	166.4	+2.8		1	144.9	-8.2
	4	168.4	+3.3		2	146.1	+5.3
	7	145.7	+2.7		3	162.4	+0.6
	2	133.3	-4.3		4	156.0	+1.6
	3	157.5	+3.0		2	145.4	-0.2
	4	167.6	+2.9		3	166.8	+1.8
	5	166.0	+2.9		2	34.9	+3.7
	6	135.3	-0.1		3	70.4	-5.4
	7	149.3	+1.8		4	57.5	-5.1
	8	172.1	+3.3		5	72.8	-4.2
	2	128.2	+2.5		6	44.1	+2.2
	3	161.4	+0.8		7	168.2	+5.3
	4	159.7	+3.0				
	5	166.9	+2.3				
	6	136.5	+0.1				
	7	146.0	+2.4				
	8	173.0	+1.9				

<sup>a</sup>  $^{13}\text{C}$  chemical shifts are given in ppm from  $\text{CS}_2$ . <sup>b</sup> The plus and minus signs mean the upfield and downfield protonation shifts, respectively.

Therefore, a  $^{13}\text{C}$  nmr study appears to be most relevant to the present study. Here we are concerned with the perturbational effect of N protonation on the  $^{13}\text{C}$  chemical shift changes for the various saturated N-heterocyclic molecules. It was found that the protonation-induced  $^{13}\text{C}$  shift depends on the orientation of the nitrogen lone-pair electrons and on the conformation of the intervening carbon skeleton. In addition to this finding, we will discuss the mechanism of electron transmission through the  $\sigma$  skeleton accompanied by nitrogen protonation. Then, based on the  $^{13}\text{C}$  chemical shift measurements, the stereospecificity of the inductive effect in the  $\sigma$  skeleton will be discussed with the aid of CNDO MO calculations.

### Experimental Section

(a)  $^{13}\text{C}$  Nmr Spectral Measurements. All  $^{13}\text{C}$  spectra were obtained at natural abundance in 8-mm  $\phi$  tubes with a Jeolco-C-60-HL spectrometer operating at 15.09 MHz. Complete proton decoupling was accomplished by the heteronuclear spin decoupler (Jeolco-SD-HC) and the proton irradiator (Jeolco-IS-60). All chemical shifts were determined with reference to internal cyclohexane or benzene and converted to the  $\text{CS}_2$  reference scale with the relation,  $\delta^{13}\text{C}_{\text{CS}_2} = \delta^{13}\text{C}_{\text{C}_6\text{H}_6} + 65.0 = \delta^{13}\text{C}_{\text{C}_6\text{H}_{12}} + 165.5$  ppm.

Neat liquid was used to observe TFA-induced protonation shifts except for quinuclidine (X) and 1-adamantanamine (XIII), the solid samples, for which  $\text{CDCl}_3$  solvent was employed (*ca.* 4 and 2 M, respectively).  $\text{CDCl}_3$  solvent shifts for  $^{13}\text{C}$  resonances were small compared with the protonation shifts.

(b) Materials. N-H piperidines, N-methylpiperidine, n-butylamine (XI), cyclohexylamine (XII), 1-adamantanamine (XIII), pyrrolidine (XIV), and  $\alpha$ -picoline (XV) were commercially available. 1,2-, 1,3-, and 1,4-dimethylpiperidines were synthesized by N-methylation of the N-H piperidine homolog.<sup>4</sup> Quinuclidine (X) was obtained from commercial (K and K) quinuclidine hydrochloride. Quinolinidine (IX) was prepared by hydrogenation of 5,6,7,8-tetrahydroquinoline. (We would like to thank Professor M. Ohashi for gift of this sample.)

(c)  $^{13}\text{C}$  Spectral Assignment of Free Amines. The experimental values of the carbon-13 chemical shift data are summarized in Table I for amines used in this study. Each carbon signal of piperidine, 4-methylpiperidine, N-methylpiperidine, 1,4-dimethylpiperidine, and quinuclidine was already assigned.<sup>5</sup> Assignments of the  $^{13}\text{C}$  signals of piperidine and N-methylpiperidine were also referred to the study of Roberts, *et al.*<sup>6</sup> With the aid of the sub-

(4) H. T. Clarke, H. B. Gillespie, and S. Z. Weisshaus, *J. Amer. Chem. Soc.*, **55**, 4571 (1933).

(5) I. Morishima, K. Okada, and T. Yonezawa, *Chem. Commun.*, 1535 (1970); *J. Amer. Chem. Soc.*, **93**, 3922 (1971).

(6) W. O. Crain, Jr., W. C. Wildman, and J. D. Roberts, *ibid.*, **93**, 990 (1971).

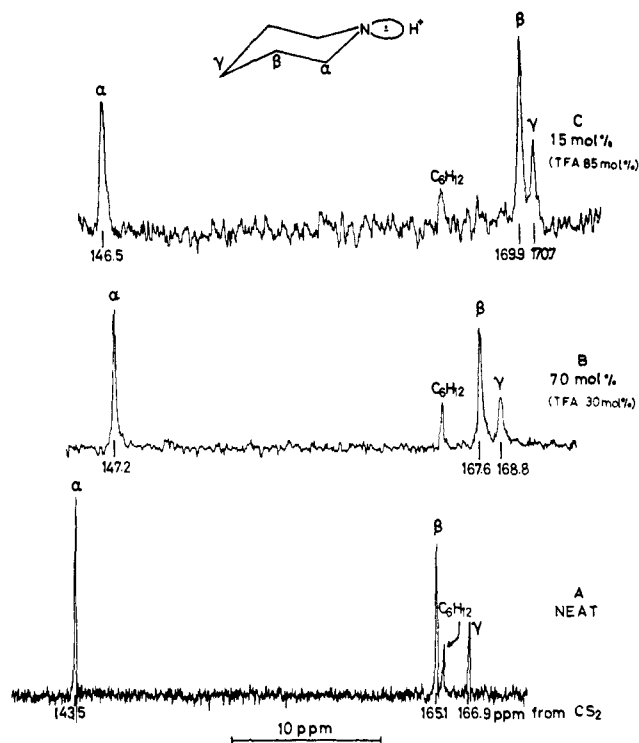


Figure 1.  $^{13}\text{C}$  nmr spectra of piperidine perturbed by the protonation in trifluoroacetic acid.

stituent parameters for the methyl group established for methylcyclohexanes by Grant, *et al.*<sup>7</sup> ( $\alpha_e \approx -6$ ,  $\beta_e \approx -9$ ,  $\gamma_e \approx 0$ , and  $\delta_e \approx 0$  ppm), signal assignment for other piperidines is feasible (see Table I). The effect of methyl substitution on the  $^{13}\text{C}$  chemical shift of the carbon skeleton for piperidines (II and III, figures are shifts from piperidine) and *N*-methylpiperidines (VI and VII, figures are shifts from *N*-methylpiperidine) is shown below. These

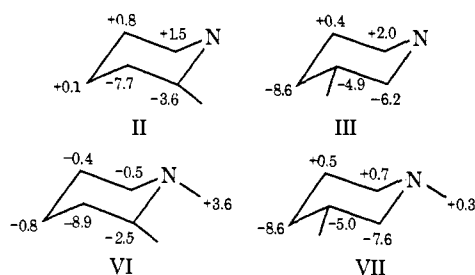


Figure 3.  $^{13}\text{C}$  chemical shifts relative to free amine ( $\Delta\delta^{13}\text{C}$ ) varying with acid-base ratios for *N*-methylpiperidine.

methyl-substituent effects correspond fairly well with Grant's substituent parameters stated above. Most of the  $^{13}\text{C}$  resonances of *N*-H piperidines and *N*-methylpiperidines were readily assigned in this way with a high degree of confidence. Assignments were also assisted by the use of the off-resonance proton decoupling technique. The signals of quinolizidine were assigned by comparison with the spectrum of 1,2-dimethylpiperidine. By utilizing the shift parameters of the  $\text{NH}_2$  substituent<sup>8</sup> and the off-resonance decoupling technique, the assignment can also be made for cyclohexylamine, *n*-butylamine, pyrrolidine, and 1-adamantanamine. The  $^{13}\text{C}$  resonances of  $\alpha$ -picoline were assigned by referring the  $\text{CH}_3$  induced shift for toluene relative to benzene.<sup>9</sup>

## Results

The  $^{13}\text{C}$  chemical shifts of various amines were measured at various concentrations in trifluoroacetic acid solution.  $^{13}\text{C}$  nmr spectra of piperidine perturbed by

(7) D. K. Dalling and D. M. Grant, *J. Amer. Chem. Soc.*, **89**, 6612 (1967).

(8) W. Horsley and H. Sternlicht, *ibid.*, **90**, 3738 (1968).

(9) H. Spiesscke and W. G. Schneider, *J. Chem. Phys.*, **35**, 731 (1961). See also D. Doddrell and J. D. Roberts, *J. Amer. Chem. Soc.*, **92**, 6839 (1970).

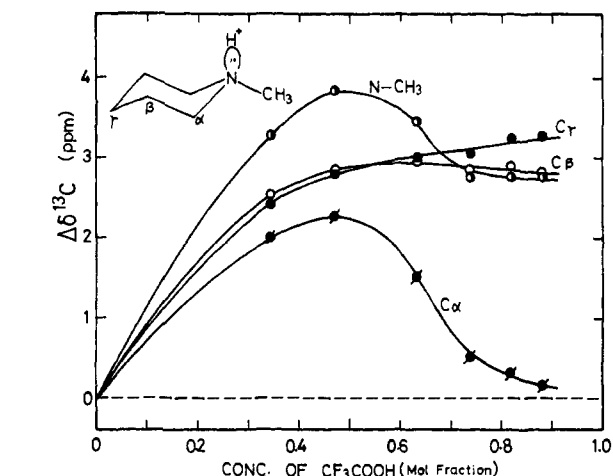


Figure 2.  $^{13}\text{C}$  chemical shifts relative to free amine ( $\Delta\delta^{13}\text{C}$ ) varying with acid-base ratios for piperidine.

the *N* protonation are shown in Figure 1. In Figures 2 and 3, the variation of  $^{13}\text{C}$  shifts induced by the addition of trifluoroacetic acid are shown for piperidine and *N*-methylpiperidine, respectively. Figures 2 and 3 also reveal that all the  $^{13}\text{C}$  signals move to higher field upon protonation and that protonation-induced  $^{13}\text{C}$  shifts exhibit saturation at the acid:base ratio of *ca.* 1:1. Similar protonation curves were obtained for other saturated amines. The  $^{13}\text{C}$  chemical shifts for completely protonated bases (with trifluoroacetic acid concentration of above 80 mol %) are summarized in Table I.

## Discussion

**A. Variations in  $^{13}\text{C}$  Chemical Shift and Electronic Structure of Saturated *N*-Heterocyclic Molecules Caused by Protonation.** Based on a theory of carbon chemical shift with the mean excitation energy approximation, Pople<sup>10</sup> predicted (1) a low-field shift for molecules with low electronic excitation energy, (2) a high-field shift if the carbon atom has high electron density, and (3) a mul-

(10) J. A. Pople, *Mol. Phys.*, **7**, 301 (1964).

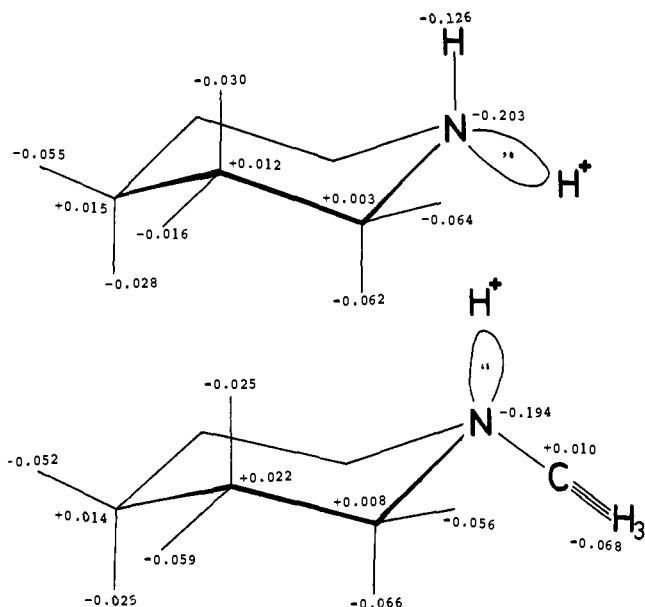


Figure 4. The changes of charge density caused by protonation (CNDO/2 calculations,  $N-H^+ = 1.032 \text{ \AA}$ ).

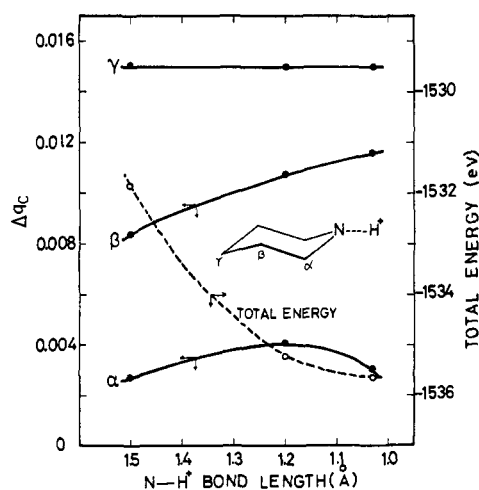


Figure 5. The protonation-induced charge density on the carbon atom of piperidine with variation of  $N-H^+$  bond length.

multiple bond effect. Indeed, several workers<sup>11</sup> have reported a good correlation between the  $^{13}\text{C}$  chemical shift and the  $\pi$ -electron density for aromatic compounds. Similar linear relation between  $^{13}\text{C}$  chemical shift and charge density on the carbon atom has also been suggested for saturated molecules.<sup>12,13</sup> It has been often believed that protonation at the nitrogen atom

(11) H. Spiesscke and W. G. Schneider, *Tetrahedron Lett.*, 468 (1961); *J. Chem. Phys.*, 35, 731 (1961); P. C. Lauterbur, *ibid.*, 43, 360 (1965); R. J. Pugmire and D. M. Grant, *J. Amer. Chem. Soc.*, 90, 4232 (1968).

(12) (a) J. M. Sichel and M. A. Whitehead, *Theor. Chim. Acta*, 5, 35 (1966); (b) T. Yonezawa, I. Morishima, and H. Kato, *Bull. Chem. Soc. Jap.*, 39, 1398 (1966).

(13) Strictly speaking, the  $^{13}\text{C}$  chemical shift on a saturated carbon skeleton is determined mainly by the factors 1 and 2 (K. Okada, I. Morishima, and T. Yonezawa, *J. Amer. Chem. Soc.*, submitted for publication). In the present study, however, we are concerned with the small amount of  $^{13}\text{C}$  shift associated with N protonation. Therefore, factor 1 may be essentially important in determining protonation-induced  $^{13}\text{C}$  shifts. In fact, the substituent effect on the shift for the carbons in various saturated molecules is plausibly reproduced by the simple CNDO/2 calculation of electron densities on the carbon (I. Morishima, *et al.*, to be submitted for publication).

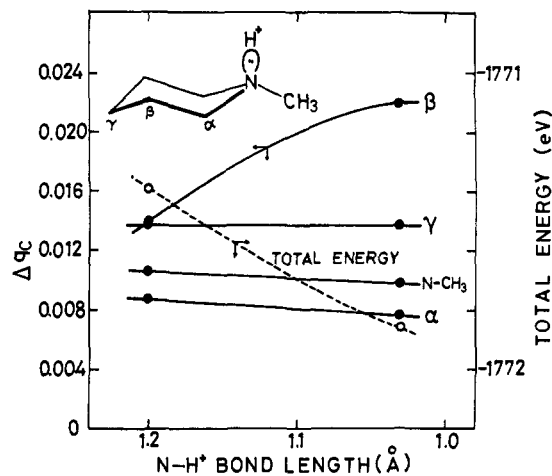
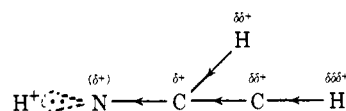


Figure 6. The protonation-induced charge density on the carbon atom of *N*-methylpiperidine.

withdraws electronic charge density from the neighboring atom in the following manner.



Consequently one will expect downfield shifts corresponding to the decreases in electron densities for all of the resonances in the  $^{13}\text{C}$  and  $^1\text{H}$  spectra. It is well known that the proton resonance of saturated amines shows a downfield shift upon protonation.<sup>14</sup> On the other hand, as Table I shows, protonation causes upfield shifts for most of the  $^{13}\text{C}$  signals. In the  $^{13}\text{C}$  magnetic resonance studies of amino acids, Horsley, *et al.*,<sup>8,15</sup> found that the  $^{13}\text{C}$  signals of  $\alpha$  carbons of the amino acids shift to a higher field upon protonation. From these results, they proposed that protonation of the amino group is accompanied by transmission of negative charge from the hydrogen through the carbons to the  $\text{NH}_3^+$  group and that the carbon charge density remains essentially constant or may actually become slightly more negative.

In order to discuss theoretically these experimental results, we have obtained changes of charge densities on carbon atoms upon protonation using the CNDO/2 MO method (Figure 4).<sup>16</sup> In both cases of piperidine and *N*-methylpiperidine, the charge densities of all of the hydrogen atoms decrease upon protonation. On the other hand, the charge densities of all of the carbon atoms increase. The increment of the electron density on the  $\alpha$ -carbon atom is smaller than that of  $\beta$ - and  $\gamma$ -carbon atoms. These results suggest that upon N protonation the carbon-hydrogen bond could be polarized to produce the  $\text{C}^--\text{H}^+$  structure and that the electron on the hydrogen atom could be transmitted through the carbon skeleton onto the positively charged nitrogen atom. Therefore, the upfield  $^{13}\text{C}$  shift resulting from protonation is attributable to the

(14) For example, L. M. Jackman and S. Sternhell, "Applications of Nuclear Magnetic Resonance Spectroscopy in Organic Chemistry," 2nd ed, Pergamon Press, London, 1967, p 180.

(15) W. Horsley and H. Sternlicht, *J. Amer. Chem. Soc.*, 92, 680 (1970).

(16) (a) J. A. Pople and G. A. Segal, *J. Chem. Phys.*, 44, 3289 (1966); (b) for the geometry of piperidine, see T. Yonezawa, I. Morishima, and Y. Ohmori, *J. Amer. Chem. Soc.*, 92, 1267 (1970).

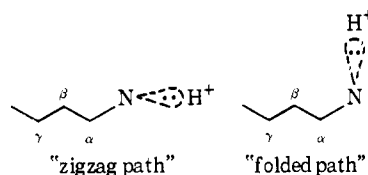
increase in the total charge densities on the carbon.<sup>13</sup> In order to discuss the peculiar behavior of the plot of <sup>13</sup>C protonation shift *vs.* concentration of trifluoroacetic acid (Figures 2 and 3), we obtained the variation of charge densities on the carbon with varying N-H<sup>+</sup> bond length (Figures 5 and 6). Of course, variation of the N-H<sup>+</sup> bond length does not directly correspond to the change in acid-base ratio. We are attempting to represent a variation in strength of an intermolecular interaction. As the N-H<sup>+</sup> distance becomes shorter, the effect of protonation becomes prominent, which may correspond to the accomplishment of protonation. From Figures 5 and 6, it is easily noticed that there are interesting features of  $\Delta q_c$ -N-H<sup>+</sup> length plots for piperidine or *N*-methylpiperidine. With variation of N-H<sup>+</sup> bond length, the charge density on the  $\alpha$  carbon has a maximum value when the N-H<sup>+</sup> length is about 1.2 Å. On the other hand, the charge density on the  $\beta$  carbon increases as the N-H<sup>+</sup> bond length increases. The electron density on the  $\gamma$  carbon remains almost constant with variation of the N-H<sup>+</sup> length from 1.5 to 1.03 Å. The observed nonlinear variation is not reproduced by the simple weighted average of charge densities for free base and protonated base.

These results of MO calculations and the chemical shift change of the  $\alpha$  carbon indicate that the charge density on the  $\alpha$  carbon increases due to the C-H bond polarization (C-H<sup>+</sup>) with respect to free amine, and when protonation is sufficient, the positive charge induced on the  $\alpha$  carbon in the manner of C<sup>δ+</sup>→N→H<sup>+</sup> will compensate for this polarization effect.

**B. Conformational Dependence of the <sup>13</sup>C Shifts Induced by N Protonation.** Inspection of Table I shows that the features of <sup>13</sup>C shifts induced by N protonation are apparently different between N-H piperidine and *N*-methylpiperidine and between 4-methylpiperidine and 1,4-dimethylpiperidine. The most striking difference is encountered for the  $\beta$  carbon, the shift for N-H piperidine being greater by about 2 ppm than that for *N*-methylpiperidine. This relation holds for 4-methyl- and 1,4-dimethylpiperidines. These different features of the <sup>13</sup>C shifts are most probably due to the structural differences between secondary and tertiary amines. These differences are also seen for the cases of quinuclidine and quinolizidine. For quinuclidine, the lone-pair electrons are in the equatorial position and the shift of the  $\alpha$  carbon is rather similar to those of *N*-methylpiperidine derivatives. Perhaps this is resulting from the fact that they are all tertiary amines. But the protonation shift of  $\beta$  carbon in quinuclidine is +4.4 ppm, closer to that in N-H piperidine derivatives (for example, +4.8 ppm for N-H piperidine) than those of *N*-methylpiperidine derivatives. On the other hand, in the case of quinolizidine, where the lone pair electrons occupy an axial position, the protonation shifts of  $\alpha$  and  $\beta$  carbons are close to those of 1,2-dimethylpiperidine.

It has been well documented<sup>5,17</sup> that the nitrogen lone-pair electrons have a greater preference for the equatorial position in N-H piperidine while those in *N*-methylpiperidines preferentially occupy an axial position. Therefore, the charge redistribution induced by

N protonation may occur through a "zigzag path" for piperidines and quinuclidine and through a "folded path" for *N*-methylpiperidines and quinolizidine. This

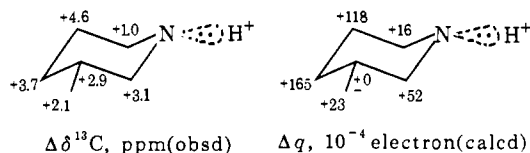


difference in the lone-pair orientation could be responsible for the different features of <sup>13</sup>C shifts induced by N protonation.

It has also to be noted in Table I that there is an alternation effect in the N-protonation <sup>13</sup>C shifts for *n*-butylamine; protonation shifts are in the order of C<sub>α</sub> < C<sub>β</sub>, C<sub>β</sub> > C<sub>γ</sub>, C<sub>γ</sub> < C<sub>δ</sub>. Such an alternation effect is also seen for cyclohexylamine and 1-adamantanamine. These features of <sup>13</sup>C shifts induced by N protonation appear to correspond with the theoretical prediction by Pople, *et al.*<sup>3,13</sup>

**C. Effect of Methyl or Methylene Substituent on the <sup>13</sup>C Protonation Shift.** When the  $\alpha$ -carbon shifts of *n*-butylamine, cyclohexylamine, and 1-adamantanamine are compared with each other, the methylene carbon of *n*-butylamine exhibits an upfield protonation shift, but the methine carbon of cyclohexylamine shows an opposite trend. Furthermore, the  $\alpha$  carbon of 1-adamantanamine shifts downfield more prominently than that of cyclohexylamine. It may be generalized from these results that the secondary carbon (which has two directly bonded hydrogens) tends to shift downfield upon protonation more than the tertiary carbon. The quaternary carbon shows downfield protonation shift more than the tertiary carbon. This trend is also found for other amines. For example, the C<sub>5</sub> resonance of 3-methylpiperidine exhibits +4.6 ppm upfield shift, while the C<sub>3</sub> resonance shifts only +2.9 ppm. We pointed out in the preceding section that the carbon-nitrogen bond is polarized upon protonation (C-H<sup>+</sup>). These experimental results could also be understood by this mechanism. If the C-H bond is more easily polarized than the C-C bond, the carbon with fewer directly bonded hydrogen atoms should accept less negative charge density from the hydrogen atom, and therefore the carbon atom becomes positive upon protonation.

In order to substantiate these views theoretically, the changes of charge densities on the carbon atoms of 3-methylpiperidine upon protonation were calculated by the CNDO/2 MO method (see below). It is apparent



that the charge densities induced by N protonation follow the variation of <sup>13</sup>C protonation shifts. The charge density on the C<sub>3</sub> atom is not affected by protonation, quite different from C<sub>5</sub>. The present MO calculation appears to support reasonably the mechanism described above.

**D. Stereospecificity of the  $\sigma$ -Inductive Effect. A Molecular Orbital Study.** In order to substantiate

(17) T. Yonezawa, I. Morishima, and Y. Ohmori, *J. Amer. Chem. Soc.*, **92**, 1267 (1970); I. Morishima, K. Okada, M. Ohashi, and T. Yonezawa, *Chem. Commun.*, 33 (1971).

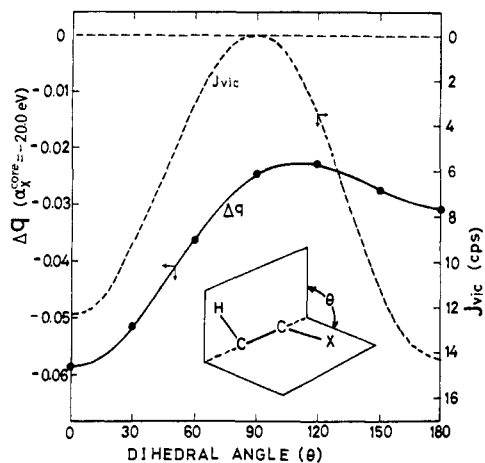


Figure 7.  $\Delta q_{H\beta}$  varying with dihedral angle  $\theta$ .

theoretically the  $\sigma$ -inductive effect<sup>18</sup> established by the <sup>13</sup>C protonation shift, we tried semiempirical MO calculations of electron charge densities on the carbon atoms for some model systems. Here we adopted the pseudo-atom approach<sup>19</sup> to introduce theoretically a  $\sigma$ -inductive effect into MO calculations. We have undertaken to see how well experimental trends can be simulated by altering pertinent atomic parameters in CNDO and INDO<sup>20</sup> methods. The parameter to be varied in CNDO or INDO is the  $1/2(I + A)$ <sup>21</sup> value employed in the diagonal elements of the core-Hamiltonian matrix. Other parameters remain unchanged in the present study. The system employed here is ethane (CH<sub>3</sub>-CH<sub>2</sub>X), where X is the pseudoatom for which the parameter variations are carried out ( $1/2(I + A)$  was varied from normal  $-7.176$  eV to a value of  $-20.0$  eV). The resulting charge density changes on the vicinal proton are given as a function of dihedral angle  $\theta$  in Figure 7. The change of charge density  $\Delta q_H$  amounts to a maximum for the cis form (dihedral angle  $\theta = 0^\circ$ ) and minimum at  $\theta = 120^\circ$ . It is of interest to note that his angular dependence of the  $\Delta q_H$  value is quite similar to that of the H-H vicinal coupling constant. (The variation of  $J_{vic}$ <sup>22</sup> is also shown in Figure 7.) The H<sub>A</sub>-H<sub>B</sub> nuclear spin-spin coupling constant  $J_{AB}$  is represented by<sup>23</sup>

$$J_{AB} = \frac{\hbar\gamma_A\gamma_B}{2\pi} \left( \frac{8\pi\beta}{3} \right)^2 S_A^2(0)S_B^2(0)\pi_{s_A s_B}$$

(18) M. J. S. Dewar and P. J. Grisdale, *J. Amer. Chem. Soc.*, **84**, 3539 (1962).

(19) G. E. Maciel and K. D. Summerhays, *ibid.*, **93**, 520 (1971).

(20) J. A. Pople, D. L. Beveridge, and P. A. Dobosh, *J. Chem. Phys.*, **47**, 2026 (1967).

(21) In CNDO/2 calculation, Fock's diagonal element  $F_{\mu\mu}$  is given by the relation

$$F_{\mu\mu} = -1/2(I_\mu + A_\mu) + [(P_{AA} - Z_A) - 1/2(P_{\mu\mu} - 1)]\gamma_{AA} + \sum_{B(\neq A)} (P_{BB} - Z_{BB})\gamma_{BB}$$

It is well known that the first term has an essential role to determine  $F_{\mu\mu}$ . If the orbital  $\phi_\mu$  contains one electron ( $P_{\mu\mu} = 1$ ) and if all atoms have zero net charge ( $P_{AA} = Z_A$ ,  $P_{BB} = Z_B$ ) the diagonal element  $F_{\mu\mu}$  becomes  $-1/2(I_\mu + A_\mu)$ . The value of  $(I + A)$  corresponds to the Mulliken-type atomic electronegativity. An atom with a large value of  $1/2(I + A)$  shows the electron-withdrawing inductive effect.

(22) A. A. Bothner-By, *Advan. Magn. Resonance*, **1**, 195 (1965).

(23) J. A. Pople and D. P. Santry, *Mol. Phys.*, **8**, 1 (1964); **9**, 301, 311 (1965).

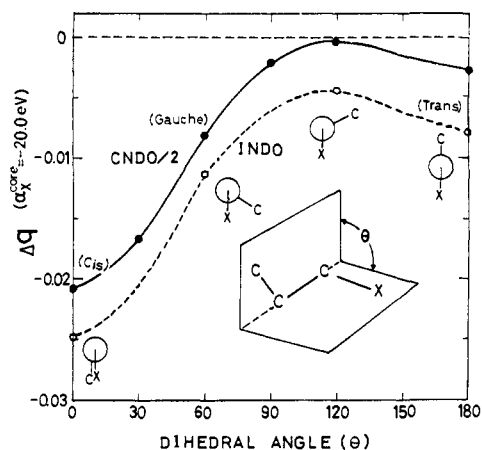


Figure 8.  $\Delta q_{C\gamma}$  varying with dihedral angle  $\theta$ .

where  $\pi_{\mu\nu}$  is the mutual polarizability

$$\pi_{\mu\nu} = 4 \sum_i^{\text{occ}} \sum_j^{\text{unocc}} (\epsilon_i - \epsilon_j)^{-1} C_{i\mu} C_{i\nu} C_{j\mu} C_{j\nu}$$

Under the simple LCAO scheme the change in the charge density on atom "s," when the Coulomb integral  $\alpha_\gamma$  is perturbed to  $\alpha_\gamma + \delta\alpha_\gamma$ , can be given by the relation<sup>24</sup>

$$\Delta q_s \approx \pi_{\gamma s} \delta\alpha_\gamma$$

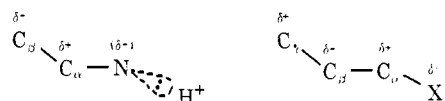
It is, therefore, reasonable to expect that there is a correlation between H-H coupling and the  $\sigma$ -inductive effect.

We have also carried out similar calculations for propane. Changes in the charge density on the  $\gamma$  carbon, when the  $1/2(I + A)$  value of  $\alpha$  hydrogen is varied from  $-7.176$  to  $-20.0$  eV, is shown in Figure 8. The  $\Delta q_{C\gamma}$  value follows an angular dependence similar to the case of  $\Delta q_H$  in ethane.  $\Delta q_{C\gamma}$  has the maximum value for the cis form and the minimum for the conformation with  $\theta = 120^\circ$ .

The stereospecificity of the protonation-induced <sup>13</sup>C shift of various amines can be reasonably recognized by the above MO calculations.<sup>25</sup> As Figure 9 shows, the protonation-induced shifts and the charge density variation in the pseudo-atom approach show the opposite trend when we compare the  $\beta$  carbon in the N-protonation model and the  $\gamma$  carbon in the pseudo-atom model. However, we are concerned here with the alternating and attenuating features of charge density in the  $\sigma$ -carbon skeleton. Therefore the stereospecific <sup>13</sup>C protonation shift may serve as a probe for studying the stereospecificity of the  $\sigma$ -inductive effect. The protonation-induced <sup>13</sup>C shift depends on the dihedral angle  $\theta$ . This angular dependence follows the trends of stereospecific  $\Delta q_{C\gamma}$  values (Figure 8). In the

(24) K. Fukui, K. Morokuma, T. Yonezawa, and C. Nagata, *Bull. Chem. Soc. Jap.*, **33**, 963 (1960).

(25) Of course, the mechanism of electron transmission is different between the nitrogen protonation and the pseudo-atom approach. These two cases can be represented schematically as follows.



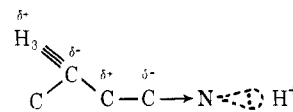
Inductive effect by N protonation      Inductive effect by the pseudo-atom approach

case of pyrrolidine, for example, the dihedral angle between the lone-pair lobe and the  $C_{\alpha}-C_{\beta}$  bond is nearly  $120^{\circ}$  and the protonation  $^{13}\text{C}$  shift is the smallest of all of the four amines (in Figure 9), which corresponds well with the MO theoretical prediction given in Figure 8. However, in the case of  $\alpha$ -picoline, where the dihedral angle between the lone-pair lobe and the  $\text{C}-\text{CH}_3$  bond is  $0^{\circ}$ , the protonation causes the largest upfield  $^{13}\text{C}$  shift for the  $\beta$  carbon. This example also corresponds with the theoretical results of the stereospecificity in the  $\sigma$ -inductive effect. For piperidine and quinuclidine, with the corresponding dihedral angle of  $180^{\circ}$ , the protonation-induced shifts for the  $\beta$  carbon are  $+4.8$  and  $+4.4$  ppm, respectively. For  $N$ -methylpiperidine and quinolizidine, with the dihedral angle of  $60^{\circ}$ , the protonation-induced shifts for the  $\beta$  carbon are  $+2.8$  and  $+2.6$  ppm, respectively. Hence the protonation-induced shifts of the  $\beta$ -carbon atoms fall in the order,  $\theta = 0^{\circ}$  (cis)  $>$   $\theta = 180^{\circ}$  (trans)  $>$   $\theta = 60^{\circ}$   $>$   $\theta = 120^{\circ}$ . The change in the charge density obtained by the pseudo-atom approach falls in the order,  $\theta = 0^{\circ}$  (cis)  $>$   $\theta = 60^{\circ}$   $>$   $\theta = 180^{\circ}$  (trans)  $>$   $\theta = 120^{\circ}$  (Figure 8).

### Conclusions

In summarizing the above results and discussion, the following conclusions may be drawn. (1) By the protonation of saturated amines the  $\text{C}-\text{H}$  bond is polarized to produce the  $\text{C}^{\delta-}-\text{H}^{\delta+}$  structure and the electron on hydrogen atom is transmitted through the carbon skeleton onto the positively charged nitrogen atom. (2) The protonation  $^{13}\text{C}$  shifts alternate and attenuate along the  $\sigma$ -carbon skeleton. These features of  $^{13}\text{C}$  shifts can be interpreted in terms of charge density variation and correspond well with alternation in the  $\sigma$ -inductive effect predicted by Pople, *et al.*<sup>3</sup>

From (1) and (2), the  $\sigma$ -inductive effect induced by N protonation may be schematically represented as follows.



(3) The  $\text{C}-\text{H}$  bond is electronically polarized more readily than the  $\text{C}-\text{C}$  bond by the inductive effect and therefore the  $\text{C}-\text{H}$  carbon has more electron density than the  $\text{C}-\text{C}$  carbon by the protonation. This may be responsible for the observed trend of protonation-induced  $^{13}\text{C}$  upfield shifts in the order of the secondary carbon  $>$  the tertiary carbon  $>$  the quaternary carbon. (4) The protonation  $^{13}\text{C}$  shifts exhibit a marked conformational dependence, which can be interpreted in terms of stereospecificity of the  $\sigma$ -inductive effect.

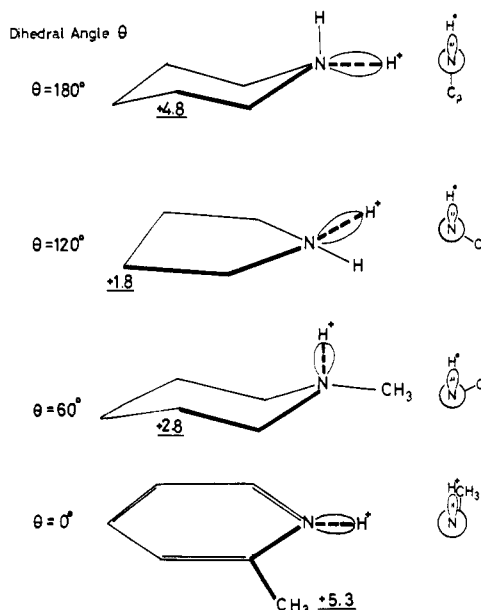


Figure 9. Stereospecific  $^{13}\text{C}$  shifts induced by protonation for several cyclic N bases (ppm).

## Conformational Mobility of *cis*-Cyclooctene-1,3,3- $d_3$ Oxide

Kenneth L. Servis\*<sup>1</sup> and Eric A. Noe

Contribution from the Department of Chemistry, University of Southern California, University Park, Los Angeles, California 90007. Received June 30, 1972

**Abstract:** Ring inversion in *cis*-cyclooctene-1,3,3- $d_3$  oxide was studied by means of low-temperature nmr spectroscopy. A single process, with a free energy of activation of 8.0 kcal/mol at  $-120^{\circ}$ , was observed. The results are interpreted in terms of a boat-chair conformation.

The transannular reactions of medium-ring compounds have been the subject of a number of investigations,<sup>2,3</sup> but frequently the presence of a specific

ring conformation has not been included in the mechanistic considerations. One of the best known of these reactions is the formolysis of *cis*-cyclooctene oxide, which gives *cis*-1,4-cyclooctanediol (23–30%), *trans*-1,2-cyclooctanediol (5–19%), 3-cycloocten-1-ol (11%), 4-cycloocten-1-ol (4%), and traces of other compounds.<sup>2b</sup> We have carried out a study of the temperature dependence of the nmr spectrum of *cis*-cyclooctene-1,3,3- $d_3$  oxide in order to obtain information about the confor-

(1) Alfred P. Sloan Research Fellow, 1969–1971.

(2) For reviews, see (a) V. Prelog and J. G. Traynham, in "Molecular Rearrangements," P. de Mayo, Ed., Interscience, New York, N. Y., 1963, Chapter 9; (b) A. C. Cope, M. M. Martin, and M. A. McKervey, *Quart. Rev., Chem. Soc.*, **20**, 148 (1966).

(3) J. G. Traynham and DeWitt B. Stone, Jr., *J. Org. Chem.*, **35**, 2025 (1970), and references therein.